DMD Fast Forward. Published on May 30, 2007 as doi:10.1124/dmd.106.014209

A minimal physiological model of thiopental distribution kinetics based on a multiple indicator approach

Michael Weiss, Tom C. Krejcie, Michael J. Avram

Section of Pharmacokinetics, Department of Pharmacology,

Martin Luther University Halle-Wittenberg, Halle, Germany (MW)

Department of Anesthesiology and the Mary Beth Donnelley Clinical Pharmacology Core Facility, Feinberg School of Medicine, Northwestern University, Chicago, IL (TCK, MJA)

Running Title: Thiopental distribution kinetics

Address correspondence to:

Michael Weiss, Ph.D.

Section of Pharmacokinetics

Department of Pharmacology

Martin Luther University Halle-Wittenberg

D-06097 Halle (Saale), Germany

Telephone: +49-345-5571657; Fax: +49-345-5571835;

E-mail: michael.weiss@medizin.uni-halle.de)

Number of:

Text pages	13
Tables	2
Figures	8
References	29
Words in the Abstract	194
Words in the Introduction	359
Words in the Discussion	1538

Abbreviations:

FT, fat tissues; NFT, non-fat tissues; TTD, transit time density

DMD Fast Forward. Published on May 30, 2007 as DOI: 10.1124/dmd.106.014209
This article has not been copyedited and formatted. The final version may differ from this version.

Abstract

Currently available models of thiopental disposition kinetics using only plasma concentration-time data neglect the influence of intratissue diffusion and provide no direct information on tissue partitioning in individual subjects. Our approach was based on a lumped-organ recirculatory model that has recently been applied to unbound compounds. The goal was to find the simplest model that accounts for the heterogeneity in tissue partition coefficients and accurately describes initial distribution kinetics of thiopental in dogs. To ensure identifiability of the underlying axially distributed capillary-tissue exchange model, simultaneously measured disposition data of the vascular indicator, ICG, and the marker of whole-body water, antipyrine, were analyzed together with those of thiopental. A model obtained by grouping the systemic organs in two subsystems containing fat and non-fat tissues, successfully described all data and allowed an accurate estimation of model parameters. The estimated tissue partition coefficients were in accordance with those measured in rats. Due to the effect of tissue binding, the diffusional equilibration time characterizing intratissue distribution of thiopental is longer than that of antipyrine. The approach could potentially be used in clinical pharmacokinetics and could increase our understanding of the effect of obesity on the disposition kinetics of lipid-soluble drugs.

It has long been a goal to understand the determinants of the distribution kinetics of intravenous anesthetics, such as thiopental, and to relate them to the duration of narcosis (Shideman et al., 1953; Brodie et al., 1952; Price, 1960). Now it is well recognized that modeling of drug distribution kinetics within the first 2 min (front-end kinetics) is of special importance (Krejcie and Avram, 1999; Avram and Krejcie, 2003). Recirculatory models with a chain of compartmental subsystems that adequately characterize pulmonary first pass distribution and initial mixing have been successfully applied to thiopental kinetics (Avram et al., 2002). These models can explain the effect of changes in cardiac output but do not account for the role of tissue partitioning and intratissue diffusion as determinants of systemic distribution kinetics of thiopental. Physiologically based models, in contrast, are very useful in explaining the effect of various physiological and anatomical factors on thiopental disposition using model simulation (Wada et al., 1997). However, they are far too complex to be fitted to plasma concentration-time data. To better understand the physiological determinants of thiopental kinetics in a clinical setting we need a model that is able to describe both front-end and disposition kinetics with parameters that can be estimated on the basis of plasma concentration-time data. Accordingly, we have recently developed a minimal physiological circulation model using a multiple indicator approach where the lumped organs of the systemic circulation were described by an axially distributed capillary-tissue exchange model that accounts for intratissue concentration gradients (Weiss et al., 2007). However, until now this model has only been applied to inulin and antipyrine, compounds that do not bind to tissue constituents (Weiss et al., 2006, 2007). The aim of this paper is to test the suitability of this model for the evaluation of thiopental disposition kinetics in dogs and to explain the difference between distribution kinetics of thiopental and antipyrine. We expect that tissue binding of thiopental leads to a slowing down of intratissue diffusion (Weiss, 1999). Another interesting question is whether the heterogeneity in partitioning of the lipophilic

compound thiopental in tissues will be consistent with the lumping of systemic organs into one subsystem.

Methods

Experimental Design of Multiple Indicator Experiments

The blood concentrations of the physiologic markers and drug used in the present analyses were taken from a study of the dispositions of markers of intravascular space (indocyanine green, ICG), total body water (antipyrine), and thiopental in five halothane-anesthetized male dogs, weighing 32 to 42.3 kg (36.7 $\pm$ 4.6 kg) (Avram et al., 2002) studied in this Institutional Animal Care and Use Committee-approved study. Details of the preparation and conduct of the studies have been described in detail previously (Krejcie et al., 1999; Avram et al., 2002).

Briefly stated, at time t = 0 min, 5 mg of ICG, 25 mg of antipyrine, and 100 mg of thiopental were flushed into the right atrium within 4 sec. Arterial blood samples were collected every 0.05 min for the first minute and every 0.1 min for the next minute. Subsequently, thirty arterial blood samples were drawn manually to 600 min.

Plasma ICG concentrations were measured by HPLC (Henthorn et al., 1992) as were plasma antipyrine concentrations (Krejcie et al., 1996a) and plasma thiopental concentrations (Avram and Krejcie, 1987). Plasma ICG concentrations were converted to blood concentrations by multiplying them by one minus the hematocrit. Plasma antipyrine and thiopental concentrations were converted to blood concentrations using an *in vivo* technique that corrects for partitioning into erythrocytes (Krejcie et al., 1996a, 1996b).

DMD Fast Forward. Published on May 30, 2007 as DOI: 10.1124/dmd.106.014209
This article has not been copyedited and formatted. The final version may differ from this version.

Model

Model 1

The minimal physiological circulation model has been described in detail previously (Weiss et al., 2007). Based on circulatory transport (Weiss et al., 1996; Weiss, 1998) and tissue diffusion of drugs (Weiss and Roberts, 1996), it consists of two subsystems, the pulmonary and the systemic circulation, which are characterized by transit time density (TTD) functions (Fig. 1). The lumped organ model of the systemic circulation that accounts for flow heterogeneity as well as the noninstantaneous mixing/distribution in the blood and tissue phases is characterized by the TTD $\hat{f}_s(s)$ (in the Laplace domain), whereas an empirical model (inverse Gaussian density) is used for the pulmonary circulation $\hat{f}_p(s)$. Both TTDs determine the arterial concentration-time curve after rapid bolus injection (dose D_{iv}) of the drug

$$\hat{C}(s) = \frac{D_{iv}}{Q} \frac{\hat{f}_p(s)}{1-(1-E)\hat{f}_s(s)\hat{f}_p(s)} \qquad (1)$$

where Q is cardiac output and E the extraction ratio of drug in the systemic circulation that determines the total body clearance $CL = QE$. Assuming that diffusion through the extravascular space is the rate limiting distribution process, $\hat{f}_s(s)$ is given by (Weiss and Roberts, 1996; Weiss et al., 2007)

$$\hat{f}_s(s) = \hat{f}_{B,s}[s + \frac{v}{d}\sqrt{ds}\tanh\sqrt{ds}] \qquad (2)$$

where $\hat{f}_{B,s}(s)$ denotes the Laplace transform of the TTD of vascular marker ICG, $v = V_T/V_B$

represents the tissue steady-state distribution volume (V_T) as fraction of the vascular volume (V_B) and $d = L^2/D_{eff}$ is the characteristic time constant of the radial intratissue diffusion process that is determined by the effective tissue diffusion coefficient (D_{eff}) and the characteristic diffusion path length (L). In order to apply the diffusion approach (Eq. 2) to thiopental, it is assumed that binding to tissue constituents occurs very rapidly compared with the diffusion timescale. This slows down the diffusion process, i.e., decreases D_{eff} (Crank, 1975; Weiss, 1999). The tissue distribution volume of thiopental can be expressed in terms of its blood/tissue partition coefficient K_p and the tissue volume, i.e., the distribution volume of the unbound solute antipyrine $V_{T,AP}$,

$$V_T = K_p \, V_{T,AP} \tag{3}$$

The Laplace transform of the density function of the inverse Gaussian distribution that is used as the empirical TTD function for the vascular marker across the systemic or pulmonary circulation denoted by $i = s$ or p, respectively, is

$$\hat{f}_{B,i}(s) = \exp\left\{ \frac{1}{RD_{B,i}^2} - \left[\frac{V_{B,i}/Q}{RD_{B,i}^2/2} \left(s + \frac{1}{2(V_{B,i}/Q)RD_{B,i}^2} \right) \right]^{1/2} \right\} \tag{4}$$

where $V_{B,i}$ and $RD_{B,i}^2$ are the distribution volume and the relative dispersion of the TTD of the vascular marker across subsystem i, i.e., Eq. 1 with Eq. 4 describes ICG concentrations during intravascular mixing. As noted above, Eq. 4 with parameters V_p and RD_p^2 has also been used as an empirical model for $\hat{f}_p(s)$.

DMD Fast Forward. Published on May 30, 2007 as DOI: 10.1124/dmd.106.014209
This article has not been copyedited and formatted. The final version may differ from this version.

Model 2

In order to test the importance of the heterogeneity in thiopental partition coefficients we have extended Model 1 by splitting the systemic circulation into two subsystems, grouping together tissues characterized by a low and high partition coefficient, $K_{p,NF}$ and $K_{p,F}$, respectively. For simplicity we call them "non-fat tissues" (NFT) and "fat tissues" (FT) (Fig. 1). This lumping procedure is in accordance with the finding that only these two tissue-plasma partition coefficients are needed to predict the volume of distribution at steady-state (Björkman, 2002). The systemic TTD is then given by

$$\hat{f}_s(s) = (1-q_F)\,(1-E_{NF})\,\hat{f}_{s,NF}(s) + q_F\,\hat{f}_{s,F}(s) \qquad (5)$$

where $q_F = Q_F/Q$ is the fraction of cardiac output going to FT and $E_{NF} = CL/Q_{NF}$. The TTDs of the subsystems NFT and FT are given by Eq. 2 with $\nu_{nf} = K_{p,NF}\,V_{T,AP}\,/V_B$ and $\nu_f = K_{p,F}\,V_{T,AP}\,/V_B$; while the diffusional equilibration time d_F is used as an adjustable parameter, it is assumed that d_F increases proportional to the increase in K_p (Weiss, 1999)

$$d_F = \frac{K_{p,F}}{K_{p,NF}}\,d_{NF} \qquad (6)$$

in order to minimize the number of parameters to be estimated and ensure model identifiability.

Whether the distribution kinetics is flow- or diffusion-limited can best be studied from the dependency of distribution (i.e., mixing) clearance, CL_M, on cardiac output. Applying the general definition in terms of the area under the distribution or mixing curve $C_M(t)$ in a hypothetical noneliminating system one obtains (Weiss and Pang, 1992; Weiss et al., 1996)

DMD Fast Forward. Published on May 30, 2007 as DOI: 10.1124/dmd.106.014209
This article has not been copyedited and formatted. The final version may differ from this version.

$$CL_M = \frac{D_{iv}}{AUC_M} = \frac{2Q}{RD_c^2 - 1} \quad (7)$$

as the clearance out of the vascular space after intravascular mixing is completed.

For Model 1, RD_C^2 in Eq. 7 can be replaced by RD_s^2 (Weiss et al., 2007)

$$RD_s^2 = RD_{B,s}^2 + \frac{2}{3}\frac{Q\,d_s}{V_{T,s}}\left(\frac{v_s}{1+v_s}\right)^2 \quad (8)$$

For $\frac{2}{3}\frac{Q\,d_s}{V_{T,s}}\left(\frac{v_s}{1+v_s}\right)^2 << RD_{B,s}^2$ distribution is flow-limited, i.e., CL_M increases in proportion to cardiac output

$$CL_M = \frac{2Q}{RD_{B,s}^2 - 1} \quad (9)$$

Parameter estimation

The simultaneous administration of ICG, antipyrine and thiopental (multiple indicator approach) allows the estimation of model parameters from indicator disposition data which are subsequently fixed in fitting the thiopental data. These are for ICG the parameters Q, $V_{B,p}$, $RD_{B,p}^2$, $V_{B,s}$ and $RD_{B,s}^2$ which describe the intravascular mixing process (estimated by fitting Eqs. 1 and 4 to the ICG data). From the parameters estimated by fitting Eqs. 1, 2 and 4 (with parameters V_p and RD_p^2) to the antipyrine data, only $V_{T,AP}$ (tissue water volume) is used in the thiopental model. Thus, for Model 1, five parameters V_p, RD_p^2, K_p, d and E remain to be

DMD Fast Forward. Published on May 30, 2007 as DOI: 10.1124/dmd.106.014209
This article has not been copyedited and formatted. The final version may differ from this version.

estimated by fitting Eqs.1, 2, 3 and 4 to the thiopental data. Note that V_p and RD_p^2 account for the distribution kinetics in the pulmonary circulation, K_p for tissue binding, d for diffusional tissue distribution and E for the systemic extraction of thiopental. In the case of Model 2, we have six adjustable parameters: V_p, RD_p^2, $K_{p,NF}$, $K_{p,F}$, d_{NF}, and E. For the fraction of blood flow to FT a value $q_F = 0.15$ was used (Ebling et al., 1994; Brown et al., 1997).

Since the model equation (Eq. 1) is only available in the Laplace domain, a numerical inverse Laplace transformation has to be performed to obtain the concentration-time curve in the time domain, $C(t) = L^{-1}[\hat{C}(s)]$. We implemented Talbot's algorithm into ADAPT II (D'Argenio and Schumitzky, 1997) and tested the accuracy and precision of parameter estimation using this method of numerical inverse Laplace transformation (Schalla and Weiss, 1999). Furthermore, using SCIENTIST (Micromath, Salt Lake City , UT) we made sure that other numerical Laplace inversion routines lead to the same result. All parameters were estimated using maximum likelihood analysis with the variance model

$$VAR_i = [\sigma_0 + \sigma_1 C(t_i)]^2 \qquad (10)$$

where VAR_i is the variance of the ith data point and $C(t_i)$ is the model prediction. "Goodness of fit" was assessed using the Akaike Information Criterion (AIC) and a visual examination of the distribution of residuals. The quality of parameter estimates was evaluated by their coefficients of variation (*CVs*). As criteria for evaluating the numerical identifiability of estimates, we used $CV < 0.5$ and a correlation coefficient threshold of 0.8.

Sensitivity analysis provides useful information for parameter estimations since a model parameter p may be most accurately gained at time points with a high sensitivity of $C(t_i)$ to the parameter p. The sensitivity function

DMD Fast Forward. Published on May 30, 2007 as DOI: 10.1124/dmd.106.014209
This article has not been copyedited and formatted. The final version may differ from this version.

$$S_p(t) = \frac{p}{C(t)} \frac{\partial C(t)}{\partial p} = \frac{p}{C(t)} L^{-1}\left[\frac{\partial \hat{C}(s)}{\partial p}\right] \quad (11)$$

determines the relative change in $C(t)$ caused by a small relative change in the model parameter p. Since S_p is nondimensional, it allows a comparison of results obtained for different parameters. Thus, $S_p(t)$ represents the relative importance of parameter p to model output. The sensitivity functions (Eq. 8 substituting Eq. 1) were calculated using MAPLE 8 after implementing a numerical method of inverse Laplace transformation (Schalla and Weiss, 1999).

Results

As shown previously in other dogs, the disposition kinetics of ICG (Weiss et al., 2006) and antipyrine (Weiss et al., 2007) were well described by the model (Fig. 2). To demonstrate the "goodness of fit", dogs with an AIC value that was closest to group median value was selected in all graphs ("representative fits"). The parameter estimates that were subsequently used as fixed parameters in fitting the thiopental data are listed in Table 1. These and all other parameters of ICG and antipyrine kinetics are not significantly different from those estimated in a previous study (Weiss et al., 2007). Figures 3A and 3B are representative fits of Model 1 and 2, respectively, to the thiopental data. For Model 1, this holds with exception of Dog 4, where it fails to fit the disposition curve (Fig. 4A). Model 2 significantly improved the fits to the data in 4 of the 5 dogs, as judged by their lower AIC values (Table 2). Most importantly, it also fitted the terminal phase of Dog 4 (Fig. 4B). The coefficients of variation of parameter estimates ranged from 0.5 % to 21 % for Model 1 and 1% to 44% for Model 2, suggesting a sufficient reliability of parameter estimation. Sensitivity analysis also indicated that the parameters can be reliably estimated with the present experimental design (Fig. 5). Note that the information on parameters of the pulmonary subsystem is restricted to the first minutes

after injection as shown for V_p. The parameter estimates summarized in Table 2 show that for Model 1 the equilibration time of thiopental tissue distribution is 2.6-fold longer than that of antipyrine and that the organ-averaged tissue partition coefficient is 1.49. The corresponding parameters of Model 2 that accounts for the heterogeneity in partitioning of thiopental into non-fat and fat components, are $K_{p,NF}$ = 0.89 and $K_{p,F}$ = 10.4 with $d_{,NF}$ /d_{AP} = 1.6. A key feature of Model 2 is the estimated ~ 10-fold higher partition coefficient of thiopental in fat tissue. The contributions of non-fat and fat tissues to the distribution volume of thiopental are shown in Fig. 6.

Discussion

There are three main facets of the present modeling of thiopental kinetics. First, both models (Model 1 and 2) describe the thiopental concentration versus time curve during the first two minutes after injection equally well (Figs. 3A and B) in accordance with the fact that this phase is mainly determined by the pulmonary first pass kinetics. Second, the refined model (Model 2) that accounts for heterogeneity in partition coefficients significantly improves the fit obtained with Model 1 and also describes the extremely long terminal half life in Dog 4 (Figs. 3B and 4B). Third, model identification is achieved by the multiple indicator dilution methodology using ICG as marker of vascular mixing and antipyrine to determine the tissue water volume.

Model 1

As previously shown for antipyrine (Weiss, 2007), diffusional resistance in tissue determines whole body distribution kinetics and, as suggested by theory (Crank, 1975; Weiss, 1999), tissue binding of thiopental slowed down this diffusional transport. Thus, the observed 2.5-fold increase in the relaxation time of the diffusional equilibration process, compared to that of the unbound drug antipyrine, can be explained by a decrease in the apparent tissue

diffusion coefficient since $D_{eff}/D_{eff,AP} = d_{AP}/d$ is obtained from $d = L^2/D_{eff}$. Due to lumping organs of the systemic circulation into a single subsystem, the estimated values for d and the tissue partition coefficient K_p represent measures averaged over all organs excluding the lung. If one calculates the organ mass-weighted average of thiopental tissue partition coefficients measured in 11 organs of the systemic circulation in rat (Ebling et al., 1994), one obtains a value of $K_p = 1.35$ that is well in accordance with our estimate of 1.49 ± 0.19. Note that a comparison of tissue partition coefficients between rat and dog appears justified since the successful scaling up of thiopental pharmacokinetics from rat to human (Wada et al., 1997) suggests that tissue partition coefficients show little variation among species. The estimates of the model-independent parameters CL and V_{ss} are not statistically significant different from those estimated previously with a different circulatory model (Avram et al., 2002).

Model 2

Although the lower AIC indicates a better fit for all data sets, the most striking advantage of Model 2 is that it also describes the terminal phase in Dog 4. It is not surprising that, in contrast to antipyrine, a neglect of partition coefficient heterogeneity in Model 1 is only a crude approximation for thiopental. Interestingly, lumping the systemic organs into two subsystems, NFT and FT, with different partition coefficients, $K_{p,NF}$ and $K_{p,F}$, respectively, where the tissue system FT is assumed to represent 15 % of body mass with fractional blood flow $q_F = 0.15$, is a suitable extension that solves this limitation. The estimates of $K_{p,NF}$ and $K_{p,F}$ (10.4 and 0.89) are again in reasonable agreement with thiopental organ partition coefficients measured in rats (Ebling et al., 1994). Thus, we obtain a weighted average of partition coefficients of 7.4 in the tissue group with high K_p (fat, kidney) and an average partition coefficient of 0.72 for the rest of the body (9 organs). Also our assumption of the fractional blood flow to FT is in accordance with that of $q_F = 0.17$ in rats (Ebling et al., 1994). Furthermore, a fractional blood flow to fat of 9.7 % has been reported for the dog (Brown et

al., 1997), a value of 11% has been estimated for perfusion of the slowly equilibrating compartment (Avram et al., 2002) and a value of 25% has been assumed for the tissue pool with the higher distribution volume in a circulatory compartment model of thiopental kinetics in sheep (Upton and Ludbrook, 1999). The diffusional equilibration time in non-fat tissues, d_{NF} = 11.7 min, is shorter than that in fat, d_F = 131.4 min. The latter has been calculated by means of Eq. 6, that follows from the fact that the effective diffusivity is inversely proportional to the tissue partition coefficient (Weiss, 1999).

Our model simulation (Fig. 7) showed that the maximum amount of thiopental in FT (38 % of dose) appeared with a delay of about 2 h relative to that in plasma and exceeded that in the rest of the body. This is in accordance with the observations in rats (Shideman et al., 1953) and dogs (Brodie et al., 1952).

Although we have no clear-cut explanation for the extremely high $K_{p,F}$ value of 17 corresponding to the long terminal half life in Dog 4, it cannot be excluded that this dog has a higher portion of fat tissue and since blood flow per unit weight of fat tissue is reduced in obesity (Coppack, 2005), this may have led to an overestimation of $K_{p,F}$. This means that a value of about 8 would have been obtained if the mass of fat tissue would have been doubled. After omission of Dog 4, the mean of $K_{p,F}$ (8.8 ± 1.9) is nearer to the literature value mentioned above (7.4) and the variance is reduced. The mean V_{ss} value of 61.0 ± 6.4 l is then in better agreement with that obtained with Model 1 (47.2 ± 3.5 l); however, only the V_{ss} estimated with Model 2 is correct since Model 1 did not cover the terminal phase in case of Dog 4. This is also obvious from Fig. 6. Our result is in accordance with the lumping procedure used to predict the V_{ss} of drugs (Björkman, 2002).

The effect of obesity on plasma concentration has been simulated in Fig. 8 for a dog with a 5-fold higher FT (i.e., 60% overweight), assuming that cardiac output increases proportional to body weight and q_F doubles. Obviously, due to the high capacity for thiopental uptake into fat, the slower terminal decay of plasma concentration is determined by the release of thiopental from FT. Note the similarity to thiopental disposition curves in obese patients (Jung et al., 1982). In contrast, the simulation showed only a minor effect on initial distribution, with a concentration peak that appeared about 10 seconds earlier.

If we calculate the distribution clearance of thiopental and antipyrine (Eqs. 6 and 7) as a function of cardiac output, it becomes obvious that the flow-limited approach holds (since $RD_s^2 \approx RD_{B,s}^2$) and CL_M increases linearly with Q and the slope is given by $2/(RD_{B,s}^2 - 1)$. This supports the notion that the whole body distribution of thiopental is flow-limited, as previously discussed for antipyrine (Weiss et al., 2007). Note that flow-limited distribution does not imply instantaneous tissue equilibration. As pointed out above, this process occurs with an equilibration time of 19 min (Model 1) or 12 min in NFT and 131 min in FT of Model 2, compared to a time constant of 8 min for antipyrine. If we define an apparent permeability-surface product that is determined by tissue diffusion according to $PS_{diff} = V_T/d$ (Weiss et al., 2007), flow limitation essentially means $PS_{diff} >> Q$ (Eq. 8). The similarity of the initial distribution kinetics of the two drugs (Avram et al., 2002), on the other hand, is due to nearly identical parameters of the pulmonary subsystem (Tables 1 and 2).

Our goal here was to develop a minimal physiologic model of thiopental kinetics, i.e., a conceptual model in which physical processes are described from first principles and thus captures the essence of distribution behavior in a more realistic way. The multiple indicator approach made it possible for the model parameters to be estimated from plasma concentration-time data. The most important findings are the following. First, it could be

DMD Fast Forward. Published on May 30, 2007 as DOI: 10.1124/dmd.106.014209
This article has not been copyedited and formatted. The final version may differ from this version.

shown that a slower diffusion in tissue can account for the difference in distribution kinetics between thiopental and antipyrine**.** Second, for the thiopental model the heterogeneity of organ partition coefficients has to be considered by treating fat tissue as a separate subsystem. The results suggest that it may be is possible to estimate organ-averaged tissue partition coefficients and equilibration times of tissue diffusion for thiopental without taking tissue samples, which makes the approach suitable for clinical studies. This would imply, however, a multiple indicator approach including frequent early arterial blood sampling, similar to the study by Avram et al. (2004) in healthy volunteers.

Regarding a comparison with other recirculatory models, it is not surprising that we get different answers depending on how we reduce the complexity of the system. Instead of assuming different compartmental organ models for different drugs (e.g., flow-limited vs. membrane-limited), the present model provides a unified approach that describes a continuous transition between the limiting cases of whole body distribution kinetics, i.e. from diffusion-limited ($PS_{diff} << Q$) to flow-limited ($PS_{diff} >> Q$) tissue distribution (Weiss et al., 2006, 2007). However, the price to be paid for the assumption of non-instantaneous distribution in the vascular and tissue space is the use of a vascular indicator and the lumped organ approach, respectively, i.e., the reduction of the systemic circulation to only one or two subsystems.

In conclusion, analysis of simultaneously measured disposition curves of ICG, antipyrine and thiopental in dogs allowed the estimation of physiologically meaningful kinetic parameters. The estimated partition coefficients of thiopental in adipose and non-adipose tissues are in good agreement with those obtained by direct tissue sampling in rats. Since the model is only based on plasma concentration data, it could potentially be used in clinical pharmacokinetics.

References

Avram MJ and Krejcie TC (1987) Determination of sodium pentobarbital and either sodium methohexital or sodium thiopental in plasma by high performance liquid chromatography with ultraviolet detection. *J Chromatogr B* **414:**484-491.

Avram MJ and Krejcie TC (2003) Using front-end kinetics to optimize target-controlled drug infusions. *Anesthesiology* **99:**1078-1086.

Avram MJ, Krejcie TC and Henthorn TK (2002) The concordance of early antipyrine and thiopental distribution kinetics. *J Pharmacol Exp Ther* **302:**594-600.

Avram MJ, Krejcie TC, Henthorn TK, Niemann CU (2004) Beta-adrenergic blockade affects initial drug distribution due to decreased cardiac output and altered blood flow distribution. *J Pharmacol Exp Ther* **311**:617-624.

Bjorkman S (2002) Prediction of the volume of distribution of a drug: which tissue-plasma partition coefficients are needed? *J Pharm Pharmacol* **54:**1237-1245.

Brodie BB, Bernstein E and Mark LC (1952) The role of body fat in limiting the duration of action of thiopental. *J Pharmacol Exp Ther* **105:**421-426.

Brown RB, Delp MD, Lindstedt SL, Rhomberg LR and Beliles RP (1997) Physiological parameter values for physiologically based pharmacokinetic models. *Toxicol Ind Health* **13:**407-484.

Coppack SW (2005) Adipose tissue changes in obesity. *Biochem Soc Trans* **33:**1049-1052.

Crank J (1975) *The Mathematics of Diffusion, 2nd ed.* p. 326, Oxford University Press, Oxford, UK.

D'Argenio DZ and Schumitzky A (1997) *ADAPT II User's guide: Pharmacokinetic/ Pharmacodynamic Systems Analysis Software.* Biomedical Simulations Resource, Los Angeles.

Ebling WF, Wada DR, and Stanski DR (1994) From piecewise to full physiologic pharmacokinetic modeling: Applied to thiopental disposition in the rat. *J Pharmacokin Biopharm* **22:**259-292.

Henthorn TK, Avram MJ, Krejcie TC, Shanks CA, Asada A and Kaczynski DA (1992) Minimal compartmental model of circulatory mixing of indocyanine green. *Am J Physiol* **262:**H903-H910.

Jung D, Mayersohn M, Perrier D, Calkins J and Saunders R (1982) Thiopental disposition in lean and obese patients undergoing surgery. *Anesthesiology* **56:**269-274.

Krejcie TC and Avram MJ (1999) What determines anesthetic induction dose? It's the front-end kinetics, doctor! *Anesth Analg* **89:**541-544.

Krejcie TC, Henthorn TK, Gentry WB, Niemann CU, Enders-Klein C, Shanks CA and Avram MJ (1999) Modifications of blood volume alter the disposition of markers of blood volume, extracellular fluid, and total body water. *J Pharmacol Exp Ther* **291:**1308-1316.

Krejcie TC, Henthorn TK, Niemann CU, Klein C, Gupta DK, Gentry WB, Shanks CA and Avram MJ (1996a) Recirculatory pharmacokinetic models of markers of blood, extracellular fluid and total body water administered concomitantly. *J Pharmacol Exp Ther* **278:**1050-1057.

Krejcie TC, Jacquez JA, Avram MJ, Niemann CU, Shanks CA and Henthorn TK (1996b) Use of parallel Erlang density functions to analyze first-pass pulmonary uptake of multiple indicators in dogs. *J Pharmacokin Biopharm* **24:**569-588.

Price HL (1960) A dynamic concept of the distribution of thiopental in the human body. *Anesthesiology* **21:**40-45.

Schalla M and Weiss M (1999) Pharmacokinetic curve fitting using numerical inverse Laplace transformation. *Eur J Pharm Sci*; **7:**305-309.

Shideman FE, Gould TC, Winters WD, Peterson RC and Wilner WK (1953) The distribution and in vivo rate of metabolism of thiopental. *J Pharmacol Exp Ther* **107:**368-378.

Upton RN and Ludbrook GL (1999) A model of the kinetics and dynamics of induction of anaesthesia in sheep: variable estimation for thiopental and comparison with propofol. *Br J Anaesth* **82:**890-899.

Wada DR, Bjorkman S, Ebling WF, Harashima H, Harapat SR and Stanski DR (1997) Computer simulation of the effects of alterations in blood flows and body composition on thiopental pharmacokinetics in humans. *Anesthesiology* **87:**884-899.

Weiss M (1998) Pharmacokinetics in organs and the intact body: model validation and reduction. *Eur J Pharm Sci* **7:**119-127.

Weiss M (1999) Cellular pharmacokinetics: Effects of cytoplasmic diffusion and binding on organ transit time distribution. *J Pharmacokinet Biopharm* **27:**233-255.

Weiss M and Pang KS (1992) Dynamics of drug distribution. I. Role of the second and third curve moments. *J Pharmacokinet Biopharm* **20:**253-278.

Weiss M and Roberts MS (1996) Tissue distribution kinetics as determinant of transit time dispersion of drugs in organs: application of a stochastic model to the rat hindlimb. *J Pharmacokinet Biopharm* **24:**173-196.

Weiss M, Hübner GH, Hübner GI and Teichmann W (1996) Effects of cardiac output on disposition kinetics of sorbitol: recirculatory modelling. *Br J Clin Pharmacol* **41:**261-268.

Weiss M, Krejcie TC, and Avram MJ (2006) Transit time dispersion in the pulmonary and systemic circulation: effects of cardiac output and solute diffusivity. *Am J Physiol Heart Circ Physiol* **291:**H861-870.

Weiss M, Krejcie TC and Avram MJ (2007) Circulatory transport and capillary-tissue exchange as determinants of the distribution kinetics of inulin and antipyrine in dog. *J Pharm Sci* 96: 913-926.

DMD Fast Forward. Published on May 30, 2007 as DOI: 10.1124/dmd.106.014209
This article has not been copyedited and formatted. The final version may differ from this version.

Legends to figures

Figure 1. Recirculatory model of thiopental disposition kinetics with systemic extraction ratio *E* and cardiac output *Q*. The pulmonary circulation is characterized by an inverse Gaussian transit time density function $\hat{f}_p(s)$ with pulmonary distribution volume V_p, and relative transit time dispersion RD_p^2. In its simplest form (Model 1), the transit time density function $\hat{f}_s(s)$ through the systemic circulation is based on a distributed model of tissue diffusion with vascular and extravascular distribution volumes $V_{B,s}$ and $V_{T,s}$, respectively. Advective mass transport occurs in the blood capillaries, whereas diffusive transport takes place in the extravascular space, characterized by a diffusional equilibration time d_s. Arterial blood concentration $C(t)$ is sampled after injection of a bolus dose D_{iv}. In the refined Model 2, the systemic organs are grouped into two subsystems, non-fat tissues and fat tissues, with partition coefficients $K_{p,NF}$ and $K_{p,F}$, respectively. The fraction of cardiac output that goes to fat tissues is denoted by q_F.

Figure 2. Model fits of arterial ICG (A) and antipyrine (B) concentration-time data (○) for dogs with median AIC values. The inset shows the complete disposition curve.

Figure 3. . Representative fits of Model 1 (A) and Model 2 (B) to arterial thiopental data (Dog 5). The inset shows the early concentrations.

Figure 4. The superiority of Model 2 (B) is obvious for Dog 4 where Model 1 (A) fails to fit the disposition curve.

Figure 5. Normalized sensitivity of thiopental disposition curve $C(t)$ with respect to diffusional equilibration time in non-fat tissues (d_{NF}), partition coefficients in non-fat ($K_{p,NF}$) and fat ($K_{p,F}$) tissues as well as the volume of distribution of the pulmonary circulation (V_p) (inset).

Figure 6. Contributions of non-fat (NF) and fat (F) tissues to the distribution volume of thiopental at steady state (TOT). Note the extremely high fat component of Dog 4.

Figure 7. Time course of thiopental distribution between fat and non-fat tissues in a model simulation (Model 2 using the average parameter estimates)

Figure 8. Model predictions of arterial thiopental concentrations for a normal dog (solid line) and an obese dog (dashed line) with a 5-fold higher mass of fat-tissue (60% overweight). The inset shows the effect on initial distribution.

Table 1. Parameter estimates of ICG and antipyrine. All ICG parameters and $V_{T,AP}$ are used in modeling of thiopental kinetics to describe initial mixing and tissue water volume, respectively.

	ICG			**Antipyrine**			
Dog	Q (l/min)	$V_{B,s}$ (l)	$RD^2_{B,s}$	$V_{p,AP}$ (l)	$RD^2_{p,AP}$	d_{AP} (min)	$V_{T,AP}$ (l)
1	2.15	4.94	9.49	0.99	0.059	3.58	35.7
2	4.82	3.33	1.60	1.76	0.045	6.18	45.1
3	2.59	2.65	3.11	0.90	0.072	8.15	46.4
4	3.11	3.04	3.85	1.09	0.057	11.06	43.5
5	3.18	2.17	2.71	1.13	0.057	9.55	42.8
Mean	**3.17**	**3.23**	**4.15**	**1.17**	**0.058**	**7.70**	**42.7**
SD	**1.01**	**1.05**	**3.09**	**0.34**	**0.010**	**2.92**	**4.2**

Table 2. Pharmacokinetic parameters of thiopental estimated by Model 1 and Model 2. Some parameters listed in Table 1 (Q, $V_{B,s}$, $RD_{B,s}^2$ and $V_{T,AP}$) are used as fixed parameters in parameter estimation.

Model 1									
Dog	V_p (l)	RD_p^2	d (min)	K_p		E	CL(l/min)[a]	V_{ss}(l) [b]	d/d_{AP}	AIC
1	1.06	0.081	7.7	1.53		0.046	0.100	41.7	2.15	230
2	1.78	0.056	26.0	1.42		0.035	0.168	50.2	4.21	251
3	0.99	0.084	24.8	1.67		0.094	0.243	50.0	3.04	234
4	1.20	0.061	15.8	1.20		0.066	0.207	47.7	1.43	221
5	1.19	0.064	18.2	1.65		0.047	0.149	46.2	1.91	231
Mean	**1.24**	**0.069**	**18.5**	**1.49**		**0.058**	**0.173**	**47.2**	**2.55**	**231**
SD	**0.31**	**0.013**	**7.4**	**0.19**		**0.023**	**0.055**	**3.5**	**1.10**	

Model 2										
Dog	V_p (l)	RD_p^2	d_{NF} (min)	$K_{p,NF}$	$K_{p,F}$ [c]	E_{NF}	CL(l/min) [e]	V_{ss}(l) [f]	d_{NF}/d_{AP}	AIC
1	1.06	0.081	4.34	0.975	10.85	0.046	0.085	63.4	1.21	230
2	1.83	0.02714	14.71	0.772	7.11	0.038	0.157	59.9	2.38	236
3	0.98	0.084	12.86	0.972	9.93	0.103	0.227	67.9	1.58	188
4	1.19	0.0628	9.23	0.739	17.04	0.059	0.155	119.7	0.83	166
5	1.26	0.0788	17.58	0.975	7.17	0.053	0.142	52.9	1.84	214
Mean	**1.26**	**0.067**	**11.74**	**0.887**	**10.42**	**0.060**	**0.153**	**72.8**	**1.57**	**214**
SD	**0.34**	**0.024**	**5.13**	**0.120**	**4.06**	**0.025**	**0.051**	**26.8**	**0.59**	

[a] $CL = E \times Q$

[b] $V_{ss} = V_p + V_{B,s} + K_p \times V_{T,AP}$

[c] Eq. 6

[e] $CL = E_{NF} \times 0.15 \times Q$

[f] $V_{ss} = V_p + V_{B,s} + (K_{NF} \times 0.85 + K_F \times 0.15) \times V_{T,AP}$

DMD Fast Forward. Published on May 30, 2007 as DOI: 10.1124/dmd.106.014209
This article has not been copyedited and formatted. The final version may differ from this version.

Fig.1

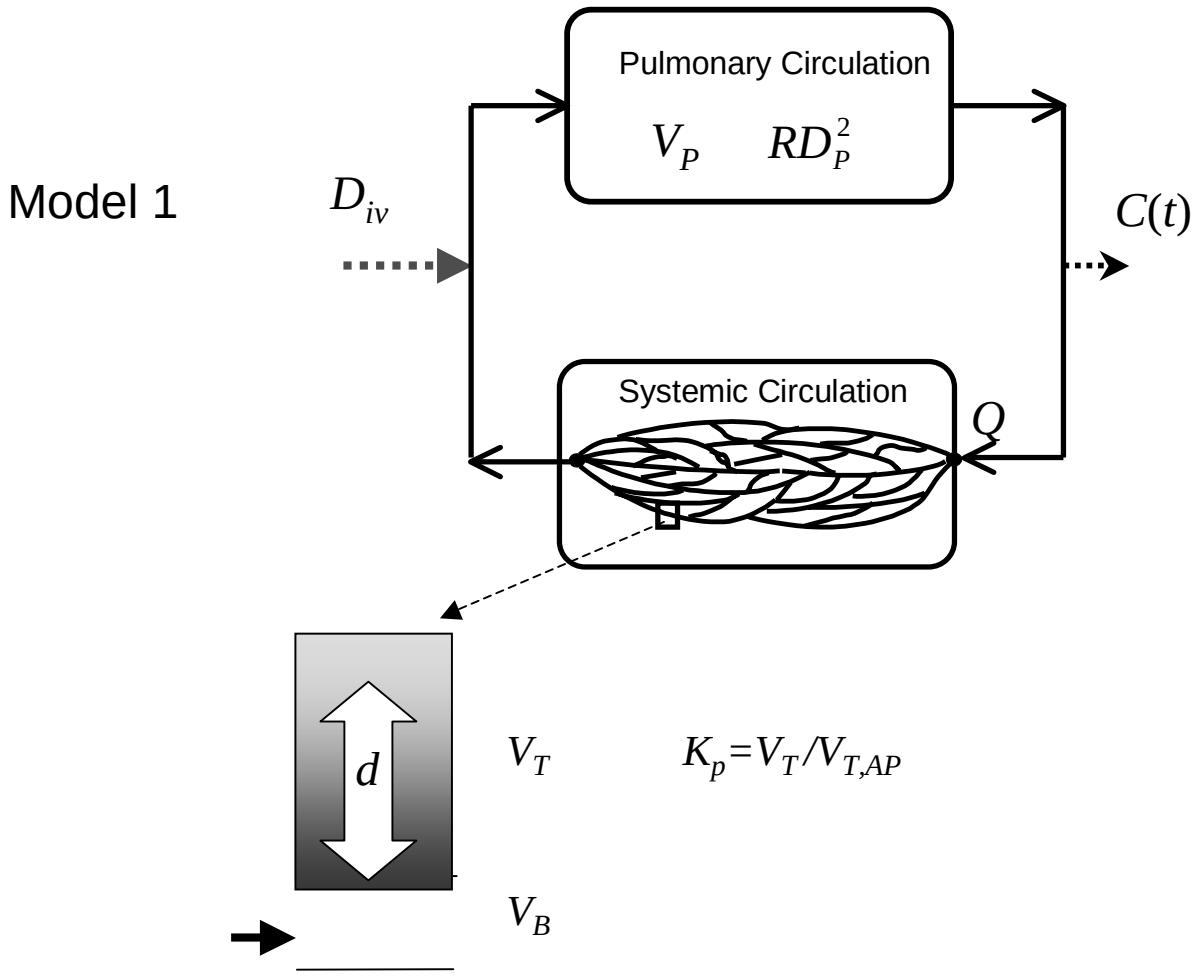

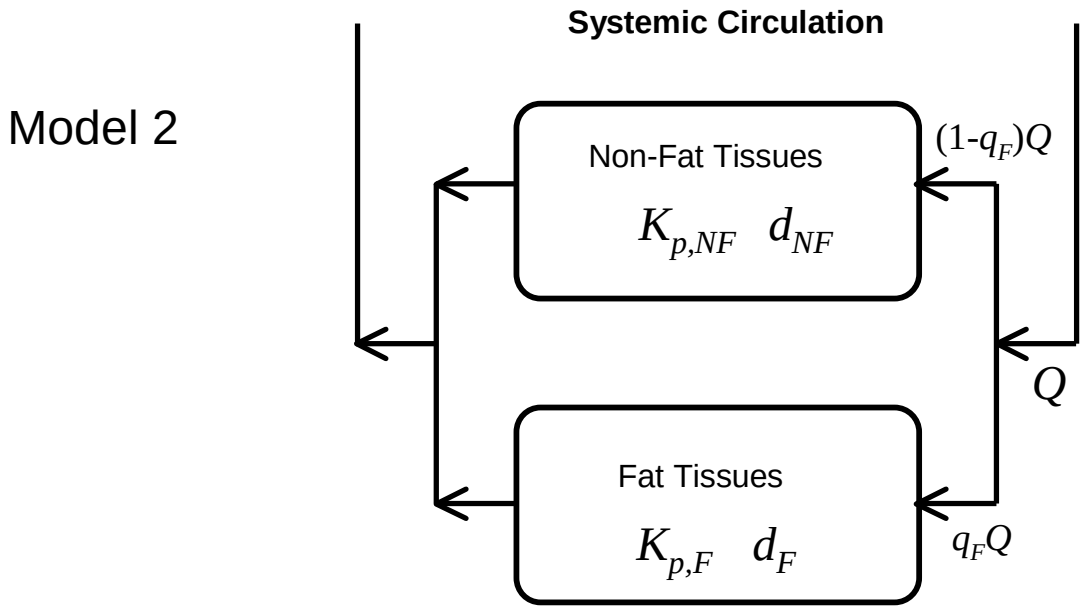

DMD Fast Forward. Published on May 30, 2007 as DOI: 10.1124/dmd.106.014209
This article has not been copyedited and formatted. The final version may differ from this version.

Fig.2

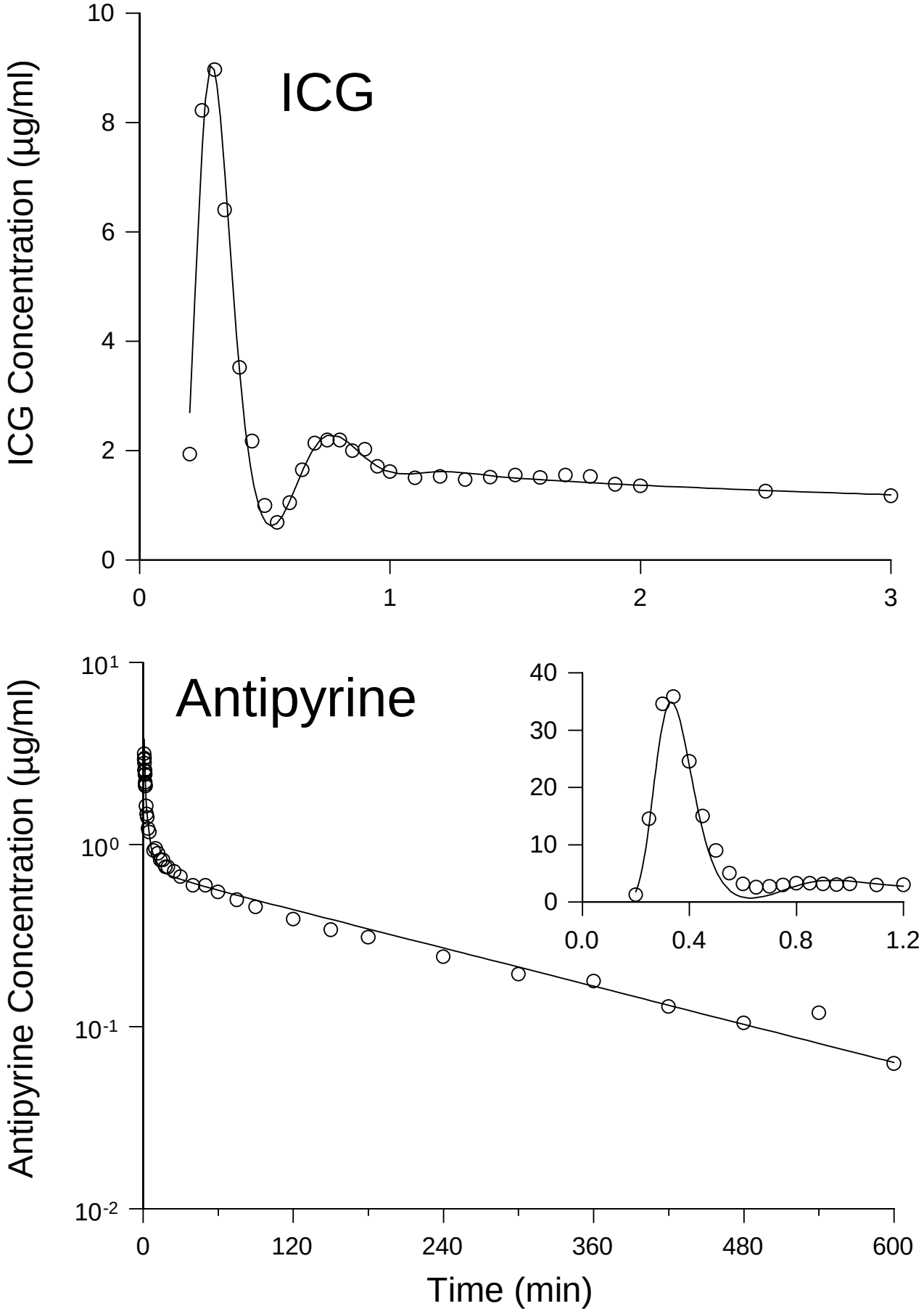

DMD Fast Forward. Published on May 30, 2007 as DOI: 10.1124/dmd.106.014209
This article has not been copyedited and formatted. The final version may differ from this version.

Fig.3

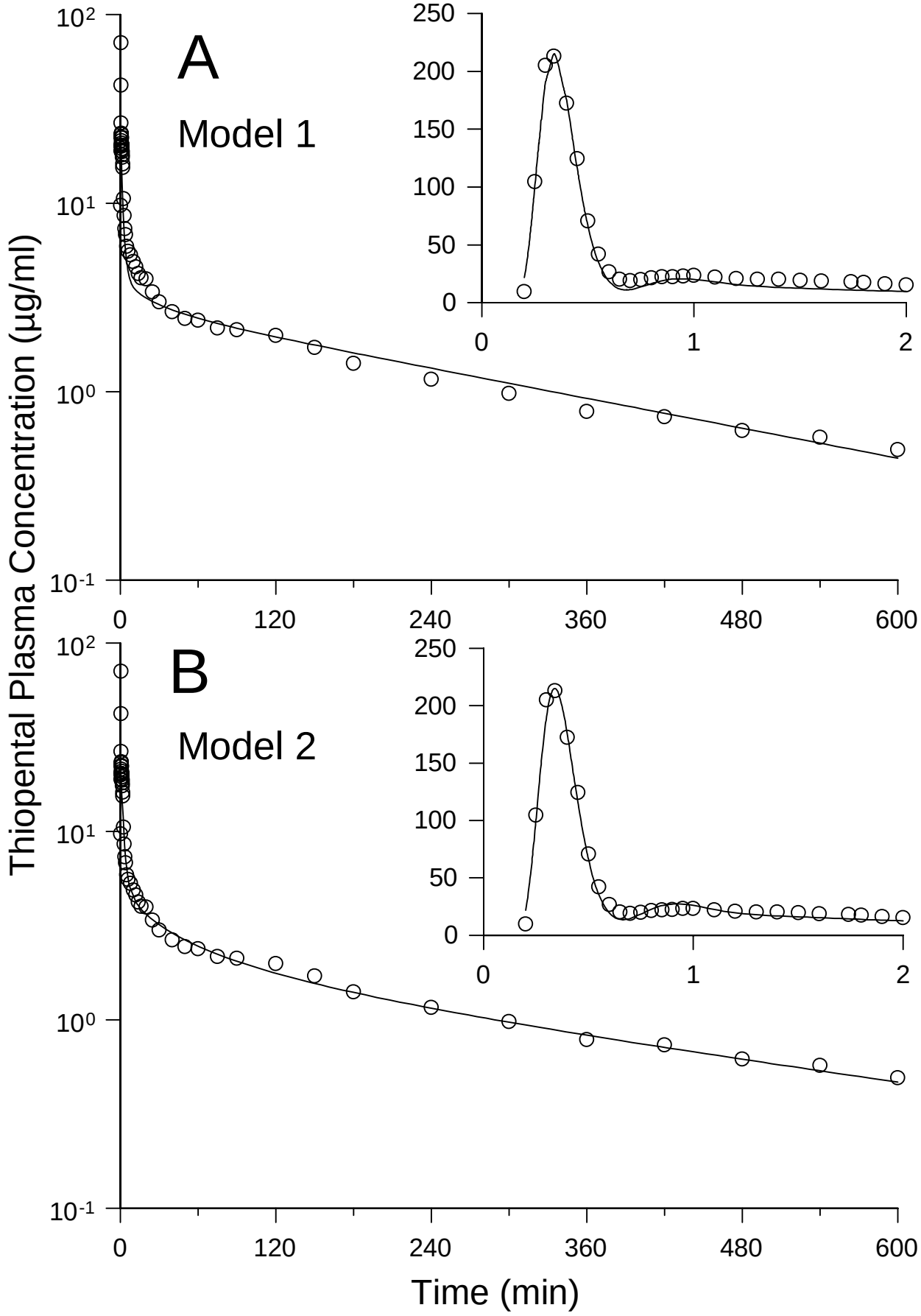

DMD Fast Forward. Published on May 30, 2007 as DOI: 10.1124/dmd.106.014209
This article has not been copyedited and formatted. The final version may differ from this version.

Fig.4

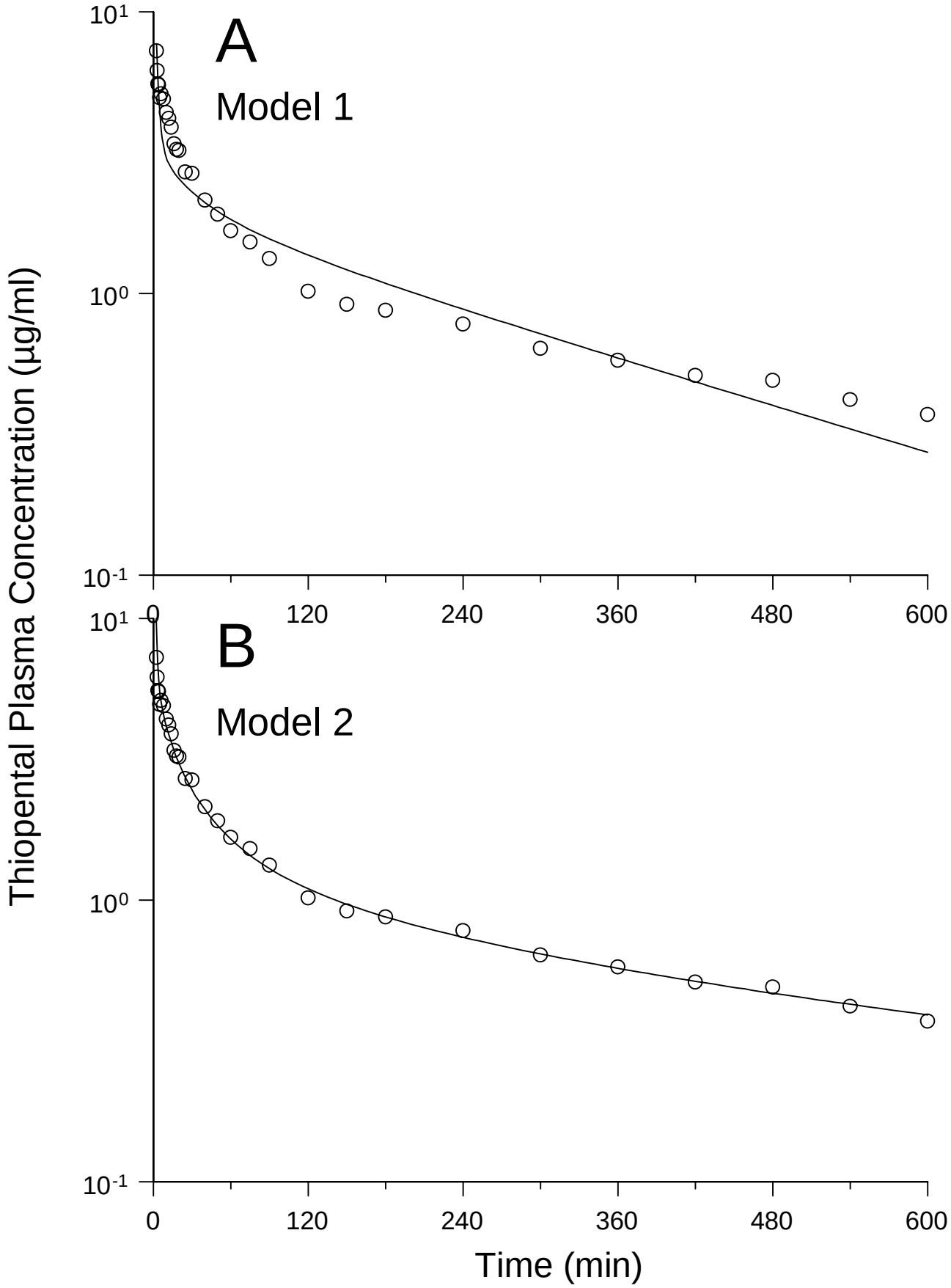

Fig.5

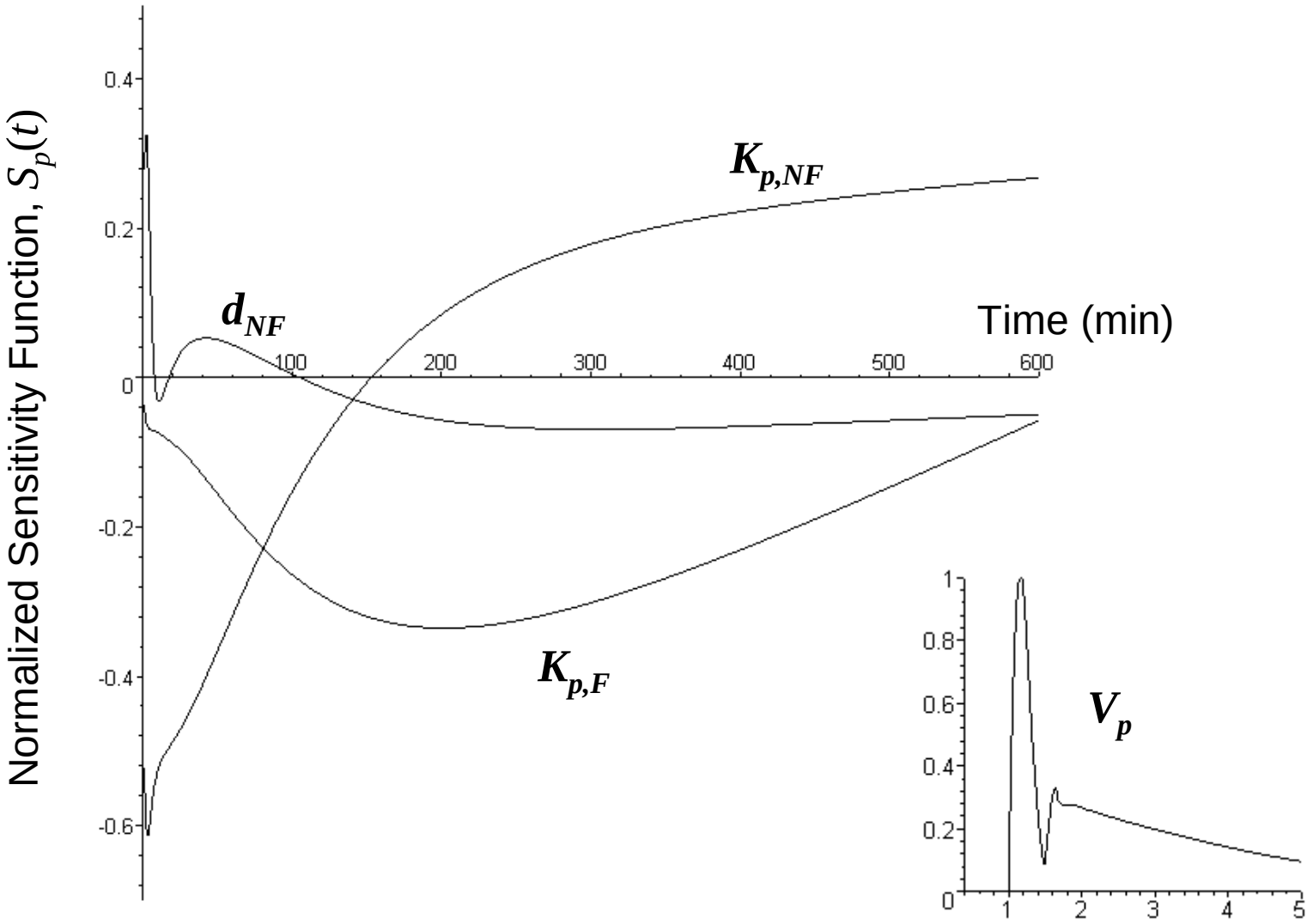

DMD Fast Forward. Published on May 30, 2007 as DOI: 10.1124/dmd.106.014209
This article has not been copyedited and formatted. The final version may differ from this version.

Fig.6

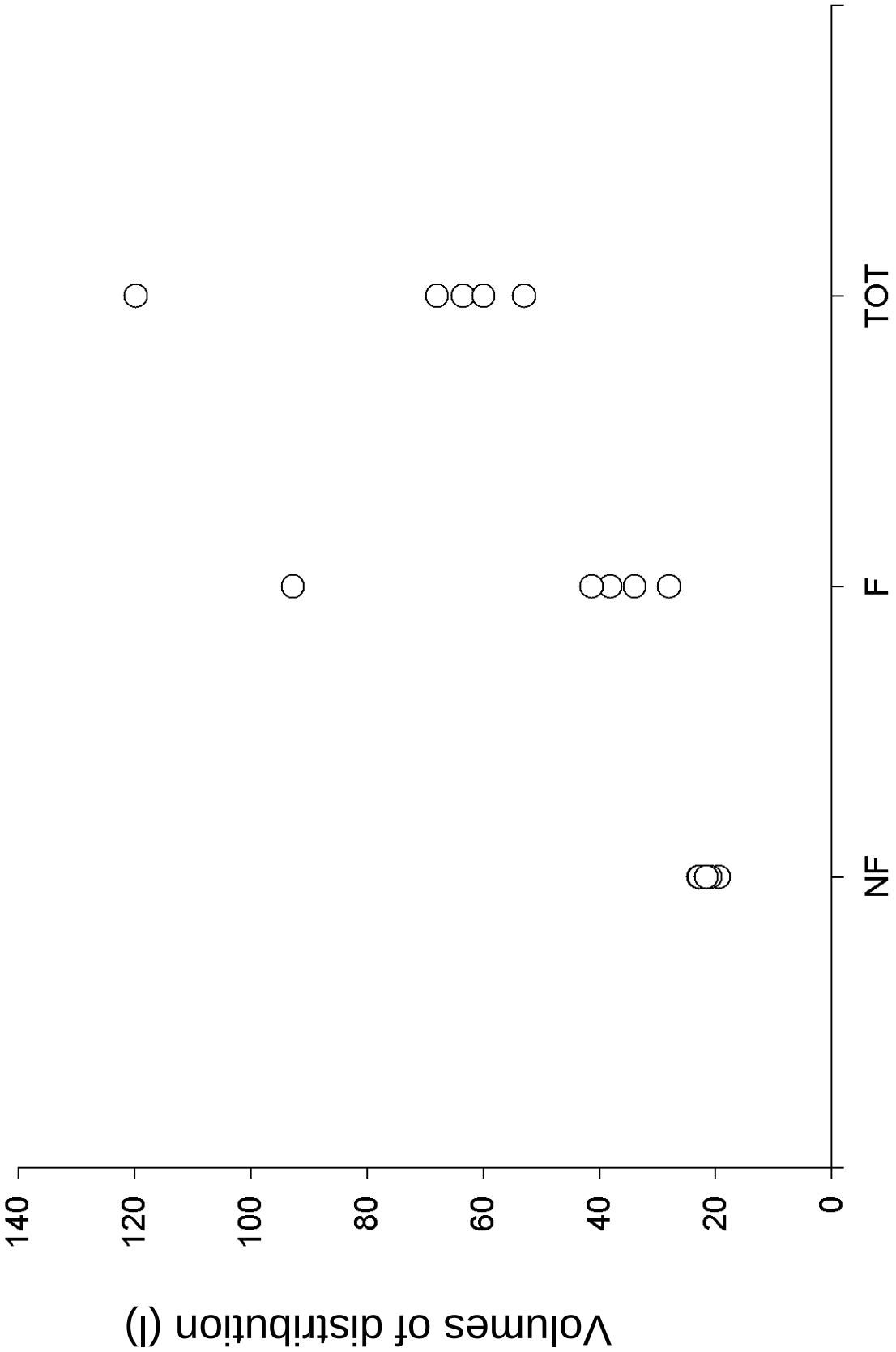

Fig.7

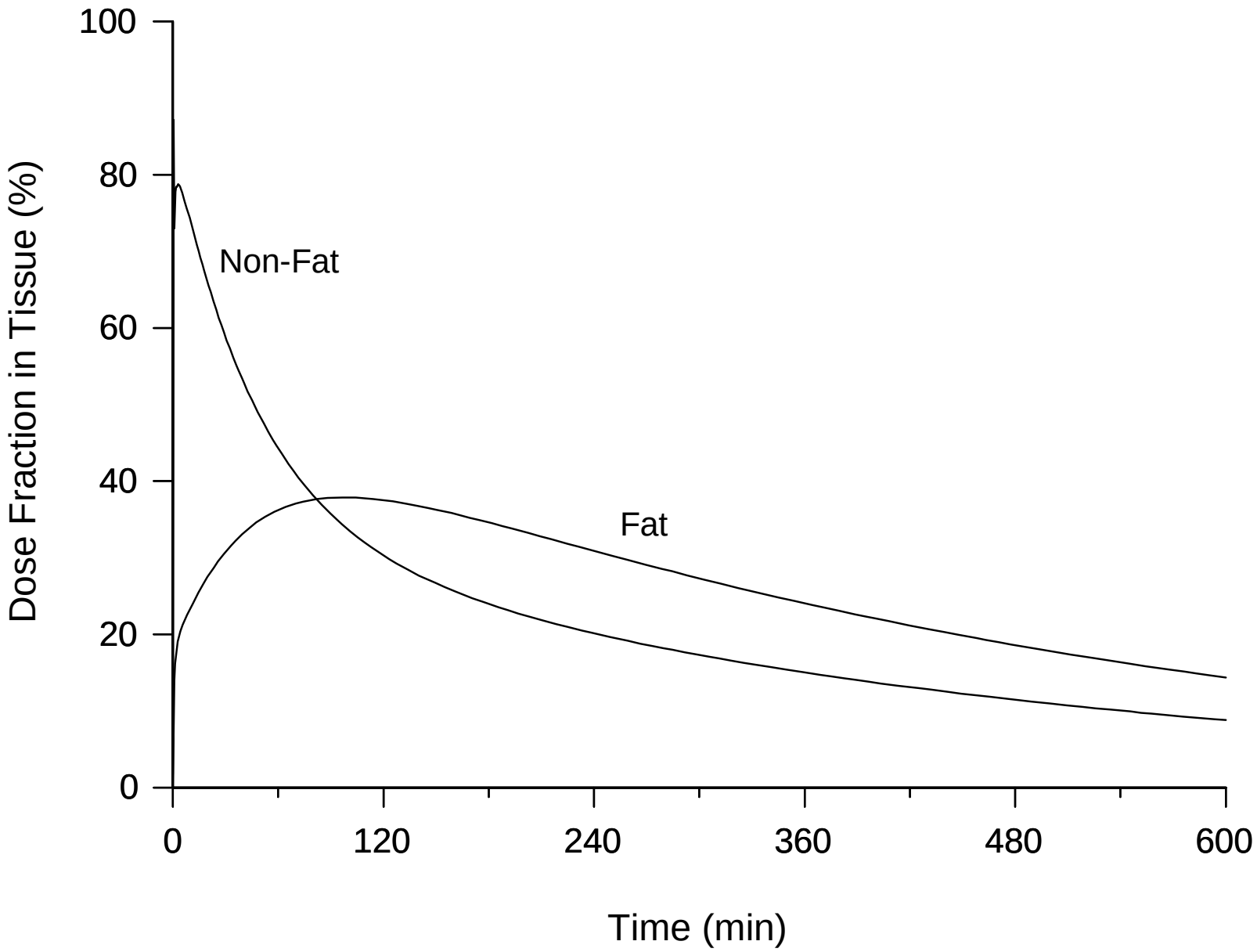

Fig.8